

Computational Analysis of Enantioselective Pd-Catalyzed α -Arylation of Ketones

Manuel Orlandi* and Giulia Licini



Cite This: *J. Org. Chem.* 2020, 85, 11511–11518



Read Online

ACCESS |



Metrics & More

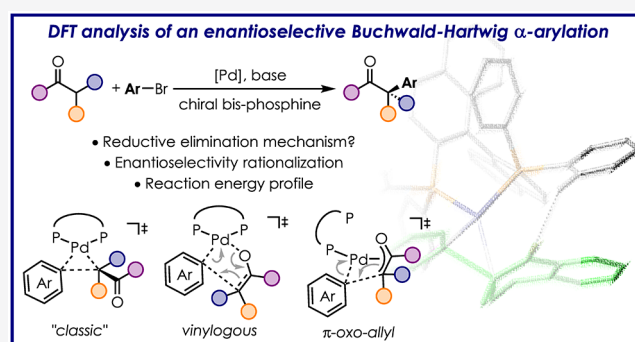


Article Recommendations



Supporting Information

ABSTRACT: The direct α -arylation of carbonyl compounds emerged over the last two decades as a straightforward method for the formation of C(sp³)–C(sp²) bonds. Mechanistic studies suggested a classical cross-coupling catalytic cycle. This consists of oxidative addition of the aryl halide (ArX) to the Pd(0)-catalyst, transmetalation of the Na- or K-enolate generated *in situ*, and subsequent reductive elimination. Even though the general reaction mechanism was thoroughly investigated, studies focusing on enantioselective variants of this transformation are rare. Here, the computational study of the [Pd(BINAP)]-catalyzed α -arylation of 2-methyltetralone with bromobenzene is reported. The whole reaction energy profile was computed and several mechanistic scenarios were investigated for the key steps of the reaction, which are the enolate transmetalation and the C–C bond-forming reductive elimination. Among the computed mechanisms, the reductive elimination from the C-bound enolate Pd complex was found to be the most favorable one, providing a good match with the stereoselectivity observed experimentally with different ligands and substrates. Detailed analysis of the stereodetermining transition structures allowed us to establish the origin of the reaction enantioselectivity.



INTRODUCTION

The first examples of direct, Pd-catalyzed α -arylation of carbonyl compounds with aryl halides^{1,2} were first reported by the groups of Buchwald and Hartwig in 1997.^{3,4} Great advances have been made in the field since then. Nowadays, carbonyl compounds ranging from ketones, aldehydes, esters, amides, and nitriles can be coupled with a plethora of aryl halides or pseudohalides with great efficiency.^{1,2} Hartwig and co-workers investigated the reaction mechanism in detail and showed that it follows the cross-coupling catalytic cycle depicted in Figure 1a.^{5–8} The reaction begins with the oxidative addition (OA) of the aryl halide ArX to the Pd(0)-catalyst. The resulting Ar-Pd-X species undergoes transmetalation (TM) with the Na- or K-enolate generated *in situ* by a suitable base (typically *t*BuONa or KHMDS). The enolate ligand can bind to the Pd center in three different modes,^{5–13} the C-bound enolate **1** being electronically more favored.^{5–8} The aryl Pd-enolate connectivity is highly dependent on sterics, and the O-bound enolate **2** becomes more favored as the hindrance of the ligand and the number of α substituents of the enolate increase.^{5–8} Finally, η^3 -bound enolates **3** (oxo- π -allylic enolates) could form upon dissociation of one of the Pd ancillary ligands (Figure 1a).^{9,14} One of the key steps of the reaction is the C–C bond-forming reductive elimination (RE), which could occur via several pathways depicted in Figure 1b. Pathway A is the direct reductive elimination between the aryl C(sp²) and the alkyl

C(sp³) of the C-bound enolate **1**. B is the vinylogous reductive elimination from the O-bound enolate **2**,^{15,16} with the C–C bond forming between the aryl C(sp²) and the alkenyl C(sp²). Pathway C is similar to mechanism A yet occurring from **3** with the enolate bound in a η^3 mode. Determining experimentally the actual reductive elimination mechanism is not trivial as pathways A, B, and C¹⁴ could all take place starting from each one of the possible enolates **1–3** by tautomerization from the most stable to the most reactive intermediate prior to the RE step.

Despite the limited knowledge about the key C–C bond-forming step in this transformation, stereoselective variants were also developed. These allow the construction of benzylic stereocenters in the α -position with respect to a carbonyl moiety, supposedly via a stereodetermining RE step.^{17–33} However, in spite of these achievements, this research area still suffers many limitations.³⁴ In this regard, the computational study of this reaction could greatly improve our understanding of its general mechanism by evaluation of the energetics of

Received: July 24, 2020

Published: July 31, 2020



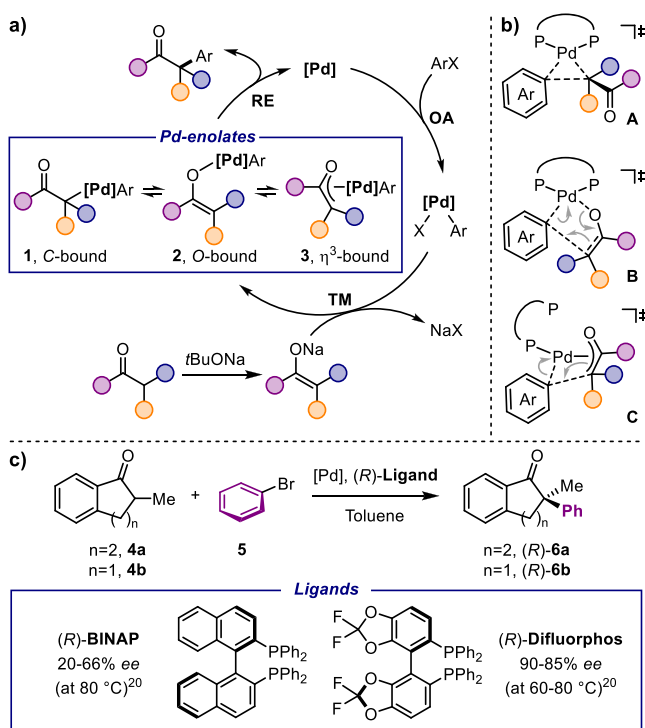


Figure 1. (a) Catalytic cycle of the α -arylation of carbonyl compounds. (b) Possible pathways for the reductive elimination step. (c) Benchmark reaction investigated in this study.

each possible pathway A–C (Figure 1b). Visualization and analysis of the diastereomeric transition structures (TSs) leading to different enantiomeric products could help in understanding the interactions responsible for the observed selectivity. This would improve the further development of catalytic systems for these transformations.^{34–37}

Computational studies of enantioselective α -arylation reactions are rare.³⁸ The first example was reported by Yamamoto and co-workers in 2011, where the authors describe Pd/Josiphos-catalyzed arylation of silyl ketene acetals in good yields and selectivities.²⁹ The authors proposed a cyclic TM TS in which the Si atom of the silyl enol ether is attacked by an acetate ligand with concomitant formation of the O–Pd bond (O-bound enolate B, Figure 1b). Based on saturation of the Pd coordination sphere, the authors excluded the tautomerization from the O- to the C-bound enolate. Hence, they computed the TSs for the RE via the vinyllogous mechanism B, which was found to proceed with an energy barrier of 27 kcal/mol. More recently, the Zhou group reported enantioselective Pd-catalyzed arylation of vinyl acetates³⁰ and silyl ketene acetals^{28,31} using a BINOL-based monophosphine ligand. The authors found that the most favorable TM pathway involved coordination of the nucleophile C=C bond by a cationic Pd-complex, with subsequent outer sphere attack of an acetate anion at the Si atom. This would directly lead to the formation of a C-bound Pd-enolate. RE would then follow with low activation barrier (13–16 kcal/mol) via the general mechanism A (Figure 1b).^{30,31} Notably, based on the weak noncovalent interactions (NCIs) present at the TS level, the authors were able to design improved versions of their ligand, leading to the improvement of the catalytic performance. These studies provide insights into the reaction mechanism of the arylation of silyl ketene acetals to give arylated products bearing tertiary stereocenters. However, because of post-

reaction racemization, these reactions are run under mild conditions, which strongly differ from those of the more widespread enantioselective direct arylation of carbonyl compounds (*vide infra*). Na- or K-enolates are expected to undergo TM via a different mechanism with respect to the one showed with Si-enolates by Zhou et al. Moreover, the relative stability of the different tautomers of Pd-enolates is dependent on the number of α -substituents of the nucleophile.^{5–8} As α -disubstituted carbonyl compounds favor the O-bound tautomer 2, one might hypothesize this preference to be translated at the TS level differently from previously studied systems.

In order to gain more insights into the reaction mechanism of the enantioselective Pd-catalyzed α -arylation of carbonyl compounds, we performed a DFT study of the [Pd((R)-BINAP)] catalyzed coupling between 2-methyltetralone 4a and bromobenzene 5 to give 6a (Figure 1c).¹⁷ The arylation of tetralones and indanones is a well-established transformation that is often used as a benchmark reaction for testing new catalytic systems.³⁴ Therefore, experimental data are available for the validation of the resulting stereochemical model. For this purpose, the reaction enantioselectivity was also computed for a different ligand and substrate: (R)-Difluorophos and 2-methylindanone 4b (Figure 1c).²⁰

RESULTS AND DISCUSSION

General Reaction Mechanism. Starting from Pd(0), π -coordination of bromobenzene 5 and subsequent OA into the C–Br bond lead to the irreversible formation of the intermediate 7 (Figure 2). The OA activation barrier is 8.26 kcal/mol. The subsequent TM step can occur by three different mechanisms: (i) bromide/enolate dissociative anion exchange, (ii) classical 4-membered cyclic transmetalation to give the O-bound Pd-enolate, and (iii) vinyllogous 6-membered cyclic transmetalation to give the C-bound Pd-enolate (Figure 2). Because of the low polarity of toluene, the formation of a cationic complex upon bromide dissociation is highly unfavored (*ca.* 42 kcal/mol, see the Supporting Information). Thus, the TM must occur between 7 and the Na-enolate 8 via cyclic TSs, TS_{TM}O or TS_{TM}C.³⁹ The latter one can exist in two diastereomeric forms (TS_{TM}CR and TS_{TM}CS, Figure 2), which at the end of the catalytic cycle lead to the formation of the two enantiomeric products (R)-6a and (S)-6a. Hence, evaluation of both the activation barrier $\Delta_{\text{TM}}G^\ddagger$ and the reaction Gibbs free energy $\Delta_{\text{TM}}G$ associated to the TM step is important. Depending on these values compared to the RE ΔG^\ddagger , the formation of the Pd-substituted stereocenter can be stereodetermining. The O-bound Pd-enolate forms with $\Delta G^\ddagger = 17.03$ kcal/mol via TS_{TM}O to give the intermediate 9 after the loss of NaBr. Formation of the C-bound enolates via TS_{TM}CR and TS_{TM}CS is much slower, with the enolate eventually leading to (S)-6a being favored ($\Delta G^\ddagger = 23.26$ and 20.42 kcal/mol, respectively). Additionally, the intermediate 9 was found to be energetically favored over the corresponding C-bound enolates (R)-10 and (S)-10 by *ca.* 8 kcal/mol. Upon transmetalation, η^3 -oxo-allyl Pd-enolates can also be easily accessed from (R)-10 and (S)-10 ($\Delta G^\ddagger = 5.9$ and 6.1 kcal/mol, respectively, not shown, see the Supporting Information). These were found to be 3–7 kcal/mol lower in energy compared to enolates 10. Nevertheless, they were still less favored than 9. This is consistent with α -disubstituted Pd-enolates typically being observed in their O-bound form.⁵ A TS directly connecting enolate 9 and (R)-10 was located (4.03

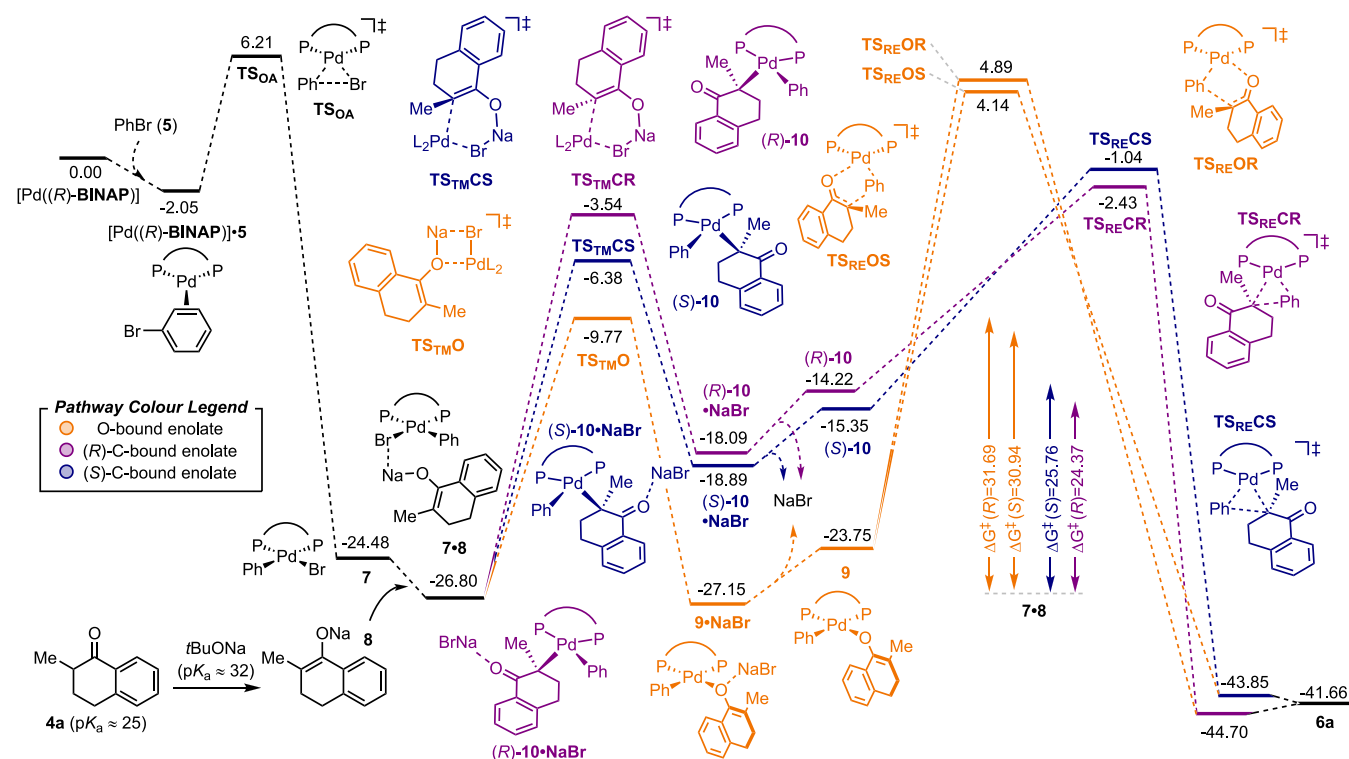


Figure 2. Reaction Gibbs free energy profile (kcal/mol) of the enantioselective α -phenylation of 2-methyltetralone **4a** catalyzed by $[\text{Pd}((R)\text{-BINAP})]$ at the $[\text{CPCM} = \text{toluene}]\text{PBE}/\text{SDD}:6\text{-}311+\text{G}(\text{d},\text{p})//\text{PBE}/\text{lan}12\text{dz}:6\text{-}31\text{G}(\text{d})$ level of theory. Different reaction pathways are highlighted in different colors (see the pathway color legend).

kcal/mol on the energy scale of Figure 2), although we were unable to find a corresponding structure between **9** and (S)-**10**. This excludes the chance for intramolecular tautomerization of **9** to **10**, as this is energetically demanding. Overall, these data suggest **9** to be the most stable Pd-enolate intermediate. The question that follows is whether it would also be the most reactive one in the next key step. TSs for the RE mechanisms depicted in Figure 1b were computed. Starting from **9**, mechanism B (Figure 1b) could occur via TS_{REOR} and TS_{REOS} , leading to (R)-**6** and (S)-**6**, respectively (orange path, Figure 2). The ΔG^\ddagger values associated to these TSs are 31.69 and 30.94 kcal/mol. This vinylogous mechanism is predicted to give low enantioselectivity toward (S)-**6a**, in contrast with the experimental evidence that (R)-**6a** is the major product when (R)-BINAP is used as the ligand. The TSs for mechanism C starting from oxo-allyl enolates show similarly high activation parameters ($\Delta G^\ddagger = 28.45$ and 33.15 kcal/mol), yet correctly predicting (R)-**6a** as the kinetically favored product (see the Supporting Information). Finally, the lowest energy pathway was found to be via mechanism A. RE occurring from C-bound enolates (R)-**10** and (S)-**10** via TS_{RECR} and TS_{RECS} shows ΔG^\ddagger as low as 24.37 and 25.76 kcal/mol, respectively (Figures 2 and 3). This suggests that despite α -disubstituted enolates bind to Pd preferentially via the O atom, this species is unproductive and needs conversion to the less-stable yet more reactive C-bound enolate **1** for the catalytic cycle to proceed.

Reaction Enantioselectivity. The computed relative energy between the TSs TS_{RECR} and TS_{RECS} is $\Delta\Delta G^\ddagger = 1.39$ kcal/mol. This value is slightly reduced to 1.16 kcal/mol when considering NCIs using the PBE-D3 functional (see the Computational Methods section). Considering the irreversibility of the RE step (ΔG ca. -28 kcal/mol, Figure 2) and

the reversible formation of (R)-**10** and (S)-**10**, the Curtin-Hammett principle can be applied.⁴⁰ Therefore, the computed $\Delta\Delta G^\ddagger$ value is in agreement with the enantioselectivity observed experimentally (66% *ee*, 1.18 kcal/mol).¹⁷ Analysis of the TSs TS_{RECR} and TS_{RECS} gives insights into the observed preference toward the product (R)-**6**. Previous work by Zhou and co-workers^{30,31} on BINOL-based monophosphine ligands showed that C–H \cdots O contacts are key features for accessing high *ee* levels. Such NCIs are also present in both TS_{RECR} and TS_{RECS} , between the carbonyl O atom and ortho-protons of the PPh₂ groups (Figure 3a). The more favored TS_{RECR} shows two C–H \cdots O interactions (2.23 and 2.31 Å), while TS_{RECS} shows only one (2.31 Å, Figure 3a). Thus, these NCIs seem to be responsible for the observed selectivity at the first glance. Aiming at a validation of our observations, we computed RE TSs also for a different ligand and substrate. (R)-Difluorophos was shown to be a ligand of choice for this transformation, providing stereoselectivity typically higher than 90% *ee* for a range of substrates.²⁰ In the case of the benchmark reaction in Figure 1c with the substrate **4a**, (R)-Difluorophos gave the product (R)-**6** in 90 or 85% *ee* (at 60 or 80 °C, respectively) corresponding to a $\Delta\Delta G^\ddagger$ range of 1.76–1.95 kcal/mol. On the other hand, the reaction performance was shown to be generally lower when contracting the substrate ring size from tetralone to indanone derivatives.²⁰ The *ee* for the reaction with (R)-BINAP and **4b** is 20% under catalytic conditions and 66% under stoichiometric conditions, corresponding to a $\Delta\Delta G^\ddagger$ range of 0.28–1.11 kcal/mol. It should be noted that catalyst decomposition was found to occur under catalytic conditions depending on the ligand, resulting in substantial variability in the observed *ee*.²⁰ Nevertheless, our stereochemical model should be able to predict the change in the reaction $\Delta\Delta G^\ddagger$ at least qualitatively,

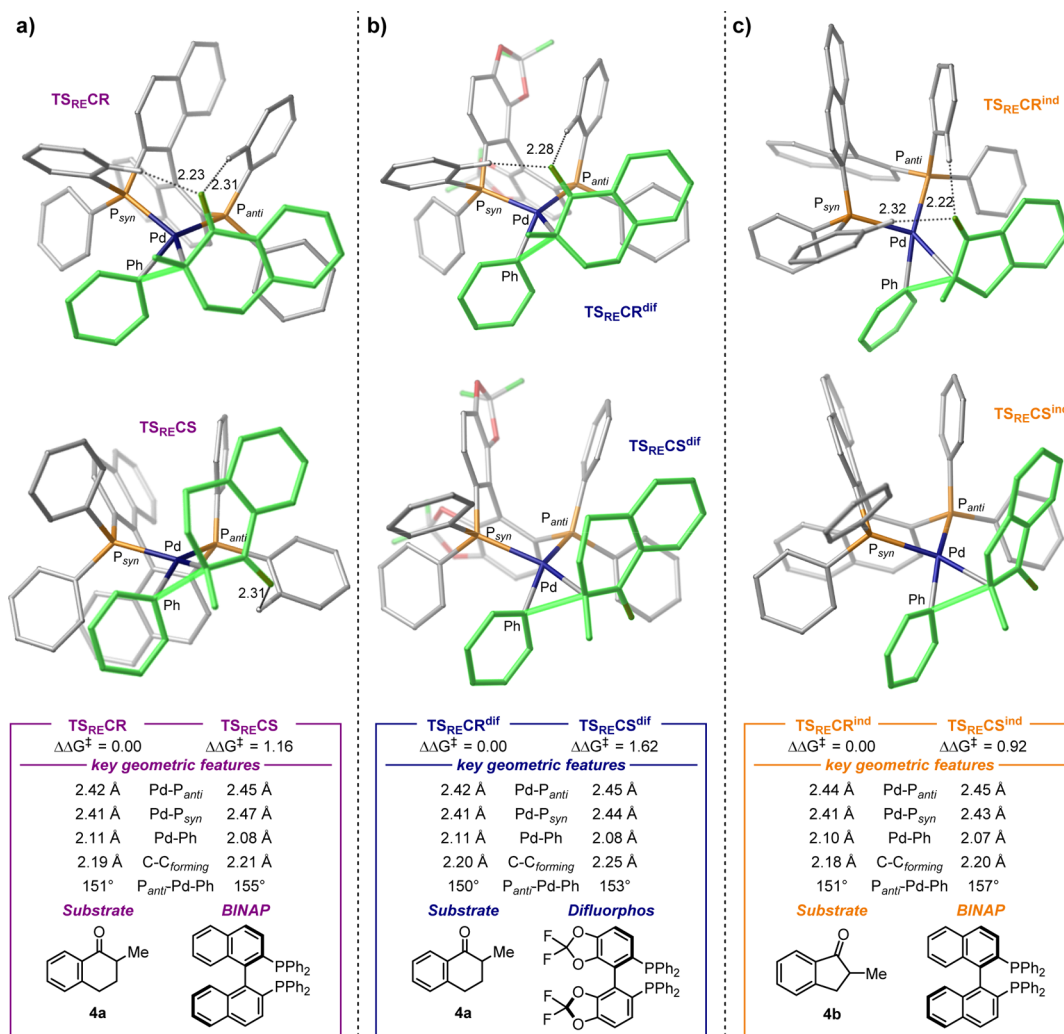


Figure 3. Computed $\Delta\Delta G^\ddagger$ values in kcal/mol and geometric features for the reaction with different ligand/substrate combinations at the [CPCM = toluene]PBE-D3/SDD:6-311+G(d,p)//PBE/lanl2dz:6-31G(d) level of theory. (a) (R)-BINAP/4a, (b) (R)-Difluorophos/4a, and (c) (R)-BINAP/4b. The phenyl and enolate ligands undergoing C–C bond formation are highlighted in green. C–H...O NCI are highlighted as black dotted lines and their values are reported in Å. All of the hydrogen atoms not involved in highlighted interactions are omitted for clarity.

if correct. The results obtained are shown in Figure 3, with the structures TS_{RECR}^{dif} and TS_{RECS}^{dif} corresponding to the TSs for the pair (R)-Difluorophos/4a and TS_{RECR}^{ind} and TS_{RECS}^{ind} for the pair (R)-BINAP/4b. Computations correctly describe the increase in $\Delta\Delta G^\ddagger$ when changing from (R)-BINAP to (R)-Difluorophos (1.62 kcal/mol Figure 3b). When considering TS_{RECR}^{ind} and TS_{RECS}^{ind}, a $\Delta\Delta G^\ddagger$ value of 0.92 kcal/mol was computed (Figure 3c). This is in agreement with the typical decrement in selectivity associated with this substrate.

Analysis of the geometry for these systems shows that the reaction selectivity and the C–H...O distances are not correlated. Despite (R)-Difluorophos gives the best selectivity, C–H...O contacts in TS_{RECR}^{dif} (2.28 and 2.28 Å) are longer than those in TS_{RECR} and TS_{RECR}^{ind} (2.23 and 2.31 Å, and 2.22 and 2.32 Å, Figure 3). Similarly, there is no trend with the NBO charges of the O and H atoms involved in the interaction (see the Supporting Information). Therefore, additional investigations were undertaken aiming at evaluating the factors affecting the stereochemical outcome. In order to gain more detailed insight into the mode of the interaction between the

ligand and the substrate, we turned to an energy decomposition analysis similar to previous studies (Figure 4a).^{41–44}

Several contributions are expected to affect the electronic energy difference between the two diastereomeric TSs ($\Delta\Delta E^\ddagger$): (i) ligand-Pd bonds, (ii) [Pd(Ph)(enolate)] Pd–C breaking bonds, (iii) ligand distortion, (iv) [Ph-enolate] distortion (which includes the forming C–C bond), (v) distortion of the Pd coordination sphere, and (vi) NCI between the ligand and the substrate/reagent and of these with the metal center.⁴⁵ The relative contribution due to the NCI between the ligand and the substrate can be evaluated by considering the TS fragmentation depicted in Figure 4a. $\Delta\Delta_{\text{Lig}} E^\ddagger$ is the electronic energy difference of the sole ligand at the TS and accounts for the relative ligand distortion. Replacing the ligand's binaphthyl and phenyl groups with H atoms in the TS results in fragments where the relative [Ph-enolate] distortion, Pd coordination sphere, P–Pd bonds, and [Pd(Ph)(enolate)] Pd–C breaking bonds are conserved.⁴⁶ Therefore, the relative energy of such fragments from the two TSs ($\Delta\Delta_{\text{Reag}} E^\ddagger$) would account for all of these contributions taken together. Subtracting $\Delta\Delta_{\text{Lig}} E^\ddagger$ and $\Delta\Delta_{\text{Reag}} E^\ddagger$ from $\Delta\Delta E^\ddagger$ gives $\Delta\Delta_{\text{NCI}} E^\ddagger$, which accounts for the relative NCI between

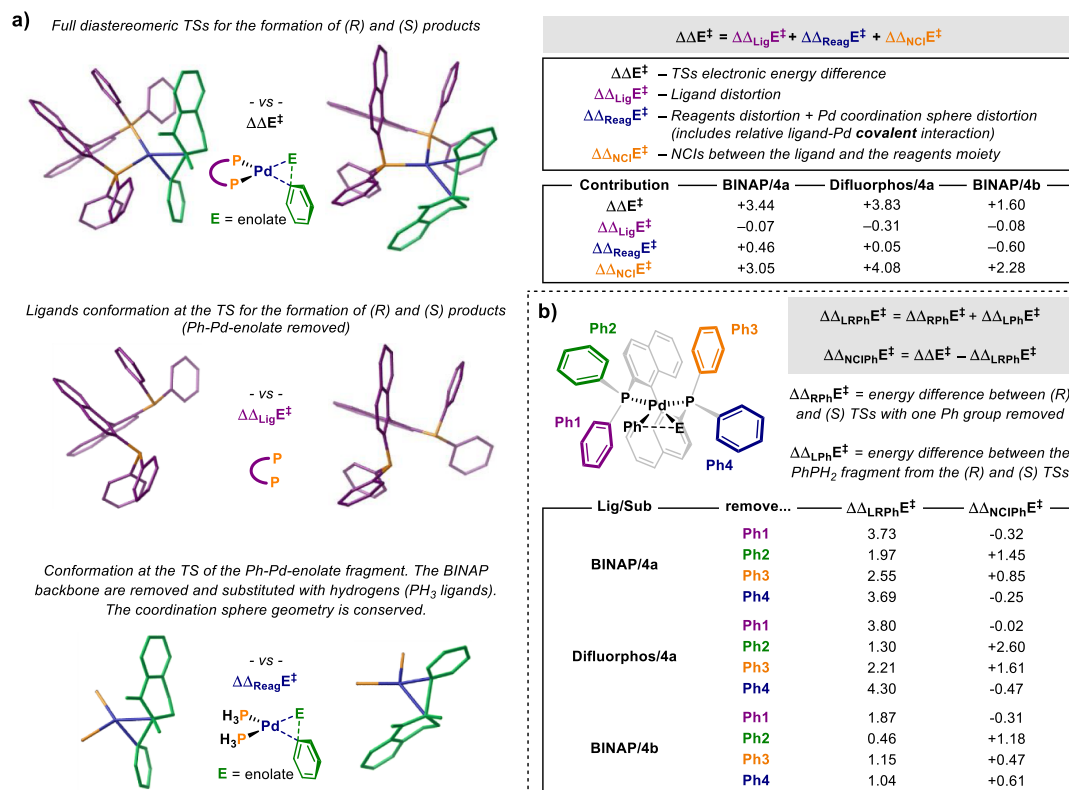


Figure 4. Energy decomposition analysis for the evaluation of the contributions affecting the reaction selectivity at the TS level. (a) General concept and evaluation of the NCI contribution given by the whole ligand. (b) Analysis of the NCI contributions given by each one of the ligand phenyl substituents.

the ligand and the [Pd(Ph)(enolate)] fragment. The values of the computed contributions for each one of the ligand/substrate combinations included in this study are reported in Figure 4. As expected, because of the rigidity of this class of bidentate ligands, $\Delta\Delta_{\text{Lig}}E^\ddagger$ was found to be small. Moreover, it was found to be always negative, that is, in favor of the minor (S)-product (-0.07 to -0.31 kcal/mol). The contribution due to the distortion of the [(PH₃)₂Pd(Ph)(enolate)] fragment ($\Delta\Delta_{\text{Reag}}E^\ddagger$) impacts the selectivity to a slightly bigger extent, even though in opposite directions depending on the substrate. $\Delta\Delta_{\text{Reag}}E^\ddagger$ is positive in the case of the tetralone derivative **4a** and negative for 2-methylindanone **4b**, suggesting a more favorable arrangement of the former substrate at the TS. The most important contribution to the computed $\Delta\Delta E^\ddagger$ is $\Delta\Delta_{\text{NCI}}E^\ddagger$. This was computed to be positive and bigger in magnitude compared to $\Delta\Delta_{\text{Lig}}E^\ddagger$ and $\Delta\Delta_{\text{Reag}}E^\ddagger$ in all the cases, indicating that the selectivity observed is mainly due to attractive⁴⁷ weak interactions between the ligand and the substrate at the TS. Such NCIs are maximized when (R)-Difluorophos is the ligand, providing $\Delta\Delta_{\text{NCI}}E^\ddagger = +4.08$ kcal/mol. A value of $+3.05$ kcal/mol was computed for the (R)-BINAP/4a combination, which further decreased for (R)-BINAP/4b ($+2.28$ kcal/mol).

$\Delta\Delta E^\ddagger$ and $\Delta\Delta_{\text{NCI}}E^\ddagger$ correlate, giving further support to the role of NCIs in the enantiodiscrimination process. Additional detail regarding such NCIs and the groups involved in the recognition event is desirable. This would provide the basis for a more rational design of improved ligands by harnessing NCIs. The effect of a specific group on the computed selectivity can be investigated by removing this from the (R) and (S)-TSs and by evaluating the change in $\Delta\Delta E^\ddagger$ associated

to this perturbation. Therefore, following the same approach described in Figure 4a, we performed an energy decomposition analysis of the TSs depicted in Figure 3 by systematically removing the Ph groups of the ligand ((R)-BINAP or (R)-Difluorophos). The results obtained are reported in Figure 4b. $\Delta\Delta_{\text{LRPh}}E^\ddagger$ is the relative distortion energy of the truncated TS and of the PhPH₂⁴⁸ residue summed. $\Delta\Delta_{\text{NCIPh}}E^\ddagger$ is the relative interaction energy due to NCIs engaging the removed Ph group and is calculated as $\Delta\Delta_{\text{NCIPh}}E^\ddagger = \Delta\Delta E^\ddagger - \Delta\Delta_{\text{LRPh}}E^\ddagger$. The previously highlighted C–H⋯O interactions are present in the favored TS of all of the systems examined (*vide infra*). Therefore, it is not surprising that Ph2 and Ph3 are the groups contributing the most to the selectivity, as these are the groups involved in the C–H⋯O contacts highlighted before. Specifically, the interactions due to these groups account for $\Delta\Delta_{\text{NCIPh}}E^\ddagger(\text{Ph2}) = 1.45$, 2.60 , and 1.18 kcal/mol and $\Delta\Delta_{\text{NCIPh}}E^\ddagger(\text{Ph3}) = 0.85$, 1.61 , and 0.47 kcal/mol for (R)-BINAP/4a, (R)-Difluorophos/4a, and (R)-BINAP/4b, respectively (Figure 4b). However, as the geometric and electronic features of these interactions do not account for the trend observed across the three systems (*vide infra*), other effects should be considered to justify the higher $\Delta\Delta_{\text{NCIPh}}E^\ddagger(\text{Ph2})$ and $\Delta\Delta_{\text{NCIPh}}E^\ddagger(\text{Ph3})$ calculated for (R)-Difluorophos/4a. We reasoned that a destabilizing interaction involving Ph2 and Ph3 could be in place in the (S)-TSs.

In both TS_{RECS} and TS_{RECS}^{dif}, the tetralone γ -methylene moiety is engaged in a CH⋯Pd interaction with the Pd occupied d_z orbital (Figure 5), which is shorter in the case of (R)-Difluorophos (2.53 Å) than for (R)-BINAP (2.63 Å). This interaction causes the substrate to be in an area occupied by Ph2 and Ph3. However, in TS_{RECS}^{dif}, the distance between the

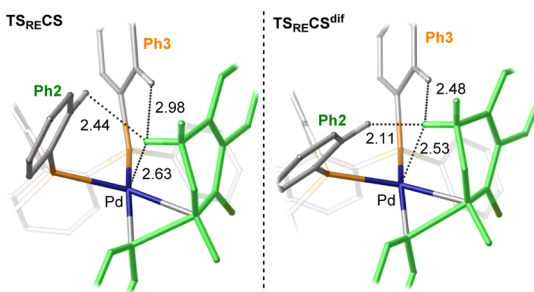


Figure 5. Detail of the structures TS_{RECS} and $\text{TS}_{\text{RECS}}^{\text{diff}}$, showing steric repulsion between the γ -methylene group of **4a** and Ph2/Ph3 in the ligand. The phenyl and enolate portions undergoing C–C bond formation are highlighted in green. H...H distances are highlighted as black dotted lines and their values are reported in Å. Hydrogen atoms not involved in highlighted interactions are omitted for clarity.

substrate CH_2 group and Ph2 is much shorter than that in TS_{RECS} . For instance, the H...H distances between the methylene of **4a** and the ortho-proton of Ph2 are 2.11 and 2.44 Å in $\text{TS}_{\text{RECS}}^{\text{diff}}$ and TS_{RECS} , respectively (Figure 5). Although the latter distance is about the sum of the van der Waals radii (2.40 Å), the former value is remarkably below this threshold, suggesting steric repulsion between these two moieties. Altogether, these data suggest that (*R*)-Difluorphos outperforms (*R*)-BINAP not only by stabilization of the favorite (*R*)-TS via NCIs but also by destabilization of the less-stable (*S*)-TS via steric repulsion. Additionally, as indanone **4b** is characterized by a contracted ring size, this substrate lacks the methylene moiety responsible for such destabilization, resulting in loss of selectivity when compared to tetralone **4a**.

CONCLUSIONS

The Pd-catalyzed α -arylation of carbonyl compounds is a fundamental reaction in transition metal catalysis. Extensive mechanistic analyses disclosed the general reaction mechanism. However, only limited information was available regarding the actual mechanism governing the formation of the product C–C bond. It was hypothesized^{5–8} that this could proceed via three possible cyclic mechanisms: (i) RE via a classic three-membered cyclic TS from a C-bound enolate; (ii) vinylogous RE from an O-bound enolate via a five-membered cyclic TS; and (iii) RE from a η^3 -bound oxo-allyl Pd-enolate. To the best of our knowledge, there were no computational studies aiming at distinguishing between these. In this work, we have computed the reaction energy profile for the general mechanism initially hypothesized by Buchwald and Hartwig (Figure 1a). Computations show that the benchmark [Pd((*R*)-BINAP)]-catalyzed coupling between 2-methyltetralone and bromobenzene proceeds via facile OA followed by TM to give C-bound enolates. Formation of the O-bound enolate is also possible and more favored, but this is shown to be an unproductive off-cycle species. RE is computed to be the stereo- and rate-determining step of the reaction, which proceeds via direct C–C bond formation from the C-bound enolates. The reaction major product was correctly computed to have (*R*)-configuration when a (*R*)-ligand is used. This is due to stabilization of the (*R*)-TS by electrostatic C–H...O contacts and destabilization of the (*S*)-TS by specific steric repulsion. Even though the attractive NCIs are similar in strength across the different ligand–substrate combinations explored; (*R*)-Difluorphos optimizes repulsive interactions, leading to higher enantioselectivity. The formulation of such a

detailed stereochemical model was possible thanks to the use of an energy decomposition analysis aimed at evaluating the contribution of each ligand's Ph substituent to the reaction selectivity. This approach was previously reported by Wheeler in the context of chiral Brønsted acid-catalyzed reactions.^{41,42} However, to the best of our knowledge, this is the first time it is applied to the rationalization of an enantioselective reaction with biaryl phosphine ligands, for which a quadrant stereo-analysis is most often used. As the development of visual-selective versions of the α -arylation of carbonyl compounds still suffers limitations,³⁴ we envision that this work will allow a more rational design of catalytic systems for this class of transformations in the future.

EXPERIMENTAL SECTION

Computational Methods. The selection of a suitable computational method capable of describing sensitive equilibria between Pd-enolate species is crucial for the success of this study. Therefore, preliminary work aiming at the identification of an appropriate functional was undertaken and is reported in the Supporting Information. The results reported were obtained by geometry optimization at the BP86/LanL2dz:6-31G(d) level of theory (LanL2dz pseudopotential for Pd, Na, and Br atoms).^{49,50} Stationary points on the potential energy surface were determined to be minima (no vibrational modes with imaginary frequency) or TSs (TS, only one mode with imaginary vibrational frequency) by vibrational analysis at the same level. Finer single point energy (SPE) calculations were performed at the PBE/SDD:6-311+(d,p) level⁵¹ with the polarizable continuum model CPCM⁵² for toluene, which is the solvent used experimentally.^{17,20} Thermal corrections were calculated from the vibrational analysis at the BP86/LanL2dz:6-31G(d) level of theory on the optimized geometries. We arbitrarily report in the text the results obtained with PBE, as these provide a better fit to the experimental data. However, other DFT methods including hybrid functionals were evaluated and found to reproduce the results obtained with the PBE functional (see the Supporting Information).

It is well-recognized that dispersion corrections are normally needed to account for NCIs. In this specific study, we found that functionals including long-range dispersion failed in reproducing the experimental distribution between the two Pd-enolate tautomeric forms (see the Supporting Information). We posit this to be due to an overestimation of the NCIs between the C-bound enolate and the Pd-complex. α -Disubstituted enolates are found in solution as O-bound tautomers **2** most likely because of steric repulsion, which seems to be underestimated in the case of long-range-corrected functionals. On the other hand, NCIs are likely to be involved in the molecular recognition process, leading to the enantiodiscrimination of the products.⁵³ Indeed, we computed the diastereomeric TSs of the reaction stereodetermining step, also adding the Grimme long-range dispersion correction GD3⁵⁴ to the PBE functional (PBE-D3/SDD:6-311+(d,p)). This provided a better fit with the experimental enantioselectivity trend for the catalyst/substrate combinations explored, suggesting the requirement for specific computational tools for the investigation of different aspects of this reaction.

ASSOCIATED CONTENT

Supporting Information

The Supporting Information is available free of charge at <https://pubs.acs.org/doi/10.1021/acs.joc.0c01768>.

Computational methods, coordinates of located structures, and corresponding thermochemical data (PDF)

AUTHOR INFORMATION

Corresponding Author

Manuel Orlandi – Department of Chemical Sciences, University of Padova, 35131 Padova, Italy; orcid.org/0000-0002-0569-6719; Email: manuel.orlandi@unipd.it

Author

Giulia Licini – Department of Chemical Sciences, University of Padova, 35131 Padova, Italy; CIRCC—Consorzio Interuniversitario per le Reattività Chimiche e la Catalisi, Padova Unit, 35131 Padova, Italy; orcid.org/0000-0001-8304-0443

Complete contact information is available at: <https://pubs.acs.org/10.1021/acs.joc.0c01768>

Notes

The authors declare no competing financial interest.

ACKNOWLEDGMENTS

Computations were performed at the HPC facility of the Computational Chemistry Community of Padova (C3P). The Department of Chemical Sciences of the University of Padova is thankfully acknowledged for the grant P-DiSC#08-BIRD2019. We thank Prof. Zonta C. and Dr. Ruchti J. for helpful discussions.

REFERENCES

- Johansson, C. C. C.; Colacot, T. J. Metal-Catalyzed α -Arylation of Carbonyl and Related Molecules: Novel Trends in C-C Bond Formation by C-H Bond Functionalization. *Angew. Chem., Int. Ed.* **2010**, *49*, 676.
- Bellina, F.; Rossi, R. Transition Metal-Catalyzed Direct Arylation of Substrates with Activated sp³-Hybridized C-H Bonds and Some of Their Synthetic Equivalents with Aryl Halides and Pseudohalides. *Chem. Rev.* **2010**, *110*, 1082.
- Palucki, M.; Buchwald, S. L. Palladium-Catalyzed α -Arylation of Ketones. *J. Am. Chem. Soc.* **1997**, *119*, 11108.
- Hamann, B. C.; Hartwig, J. F. Palladium-Catalyzed Direct α -Arylation of Ketones. Rate Acceleration by Sterically Hindered Chelating Ligands and Reductive Elimination from a Transition Metal Enolate Complex. *J. Am. Chem. Soc.* **1997**, *119*, 12382.
- Culkin, D. A.; Hartwig, J. F. C-C Bond-Forming Reductive Elimination of Ketones, Esters, and Amides from Isolated Arylpalladium(II) Enolates. *J. Am. Chem. Soc.* **2001**, *123*, 5816.
- Wolkowski, J. P.; Hartwig, J. F. Generation of Reactivity from Typically Stable Ligands: C-C Bond-Forming Reductive Elimination from Aryl Palladium(II) Complexes of Malonate Anions. *Angew. Chem., Int. Ed.* **2002**, *41*, 4289.
- Culkin, D. A.; Hartwig, J. F. Palladium-Catalyzed α -Arylation of Carbonyl Compounds and Nitriles. *Acc. Chem. Res.* **2003**, *36*, 234.
- Culkin, D. A.; Hartwig, J. F. Carbon-Carbon Bond-Forming Reductive Elimination from Arylpalladium Complexes Containing Functionalized Alkyl Groups. Influence of Ligand Steric and Electronic Properties on Structure, Stability, and Reactivity. *Organometallics* **2004**, *23*, 3398.
- Yoshimura, N.; Murahashi, S. I.; Moritani, I. A new synthesis of oxo- π -allyl- and π -allylpalladium complexes via diazoketones and vinyl diazomethanes. *J. Organomet. Chem.* **1973**, *52*, C58.
- Burkhardt, E. R.; Bergman, R. G.; Heathcock, C. H. Synthesis and reactions of nickel and palladium carbon-bound enolate complexes. *Organometallics* **1990**, *9*, 30.
- Veya, P.; Floriani, C.; Chiesi-Villa, A.; Rizzoli, C. Terminal and bridging bonding modes of the acetophenone enolate to palladium(II): the structural evidence and the insertion of isocyanides. *Organometallics* **1993**, *12*, 4899.
- Sodeoka, M.; Tokunoh, R.; Miyazaki, F.; Hagiwara, E.; Shibasaki, M. Stable Diaqua Palladium(II) Complexes of BINAP and Tol-BINAP as Highly Efficient Catalysts for Asymmetric Aldol Reactions. *Synlett* **1997**, 463.
- Fujii, A.; Hagiwara, E.; Sodeoka, M. Mechanism of Palladium Complex-Catalyzed Enantioselective Mannich-Type Reaction: Characterization of A Novel Binuclear Palladium Enolate Complex. *J. Am. Chem. Soc.* **1999**, *121*, 5450.
- At the best of our knowledge, there is no experimental evidence for the existence of η^3 -bound enolates **3**. Moreover, the reductive elimination via pathway C (Figure 1b) was experimentally ruled out for the bidentate ligand DPPBz (ref 8). However, the viability of such path could be dependent on the nature of the ancillary ligands. Therefore, this was included in this study for completeness and comparison with the more likely reaction pathways A and B. Full data regarding the reactivity of η^3 -bound enolates **3** are reported in the Supporting Information.
- Keith, J. A.; Behenna, D. C.; Mohr, J. T.; Ma, S.; Marinescu, S. C.; Oxgaard, J.; Stoltz, B. M.; Goddard, W. A. The Inner-Sphere Process in the Enantioselective Tsuji Allylation Reaction with (S)-t-Bu-phosphinooxazoline Ligands. *J. Am. Chem. Soc.* **2007**, *129*, 11876.
- Keith, J. A.; Behenna, D. C.; Sherden, N.; Mohr, J. T.; Ma, S.; Marinescu, S. C.; Nielsen, R. J.; Oxgaard, J.; Stoltz, B. M.; Goddard, W. A. The Reaction Mechanism of the Enantioselective Tsuji Allylation: Inner-Sphere and Outer-Sphere Pathways, Internal Rearrangements, and Asymmetric C-C Bond Formation. *J. Am. Chem. Soc.* **2012**, *134*, 19050.
- Åhman, J.; Wolfe, J. P.; Troutman, M. V.; Palucki, M.; Buchwald, S. L. Asymmetric Arylation of Ketone Enolates. *J. Am. Chem. Soc.* **1998**, *120*, 1918.
- Hamada, T.; Chieffi, A.; Åhman, J.; Buchwald, S. L. An Improved Catalyst for the Asymmetric Arylation of Ketone Enolates. *J. Am. Chem. Soc.* **2002**, *124*, 1261.
- Chen, G.; Kwong, F. Y.; Chan, H. O.; Yu, W.-Y.; Chan, A. S. C. Nickel-catalyzed asymmetric α -arylation of ketone enolates. *Chem. Commun.* **2006**, 1413.
- Liao, X.; Weng, Z.; Hartwig, J. F. Enantioselective α -Arylation of Ketones with Aryl Triflates Catalyzed by Difluorophos Complexes of Palladium and Nickel. *J. Am. Chem. Soc.* **2008**, *130*, 195.
- Ge, S.; Hartwig, J. F. Nickel-Catalyzed Asymmetric α -Arylation and Heteroarylation of Ketones with Chloroarenes: Effect of Halide on Selectivity, Oxidation State, and Room-Temperature Reactions. *J. Am. Chem. Soc.* **2011**, *133*, 16330.
- Spielvogel, D. J.; Buchwald, S. L. Nickel-BINAP Catalyzed Enantioselective α -Arylation of α -Substituted γ -Butyrolactones. *J. Am. Chem. Soc.* **2002**, *124*, 3500.
- Xie, X.; Chen, Y.; Ma, D. Enantioselective Arylation of 2-Methylacetoacetates Catalyzed by CuI/trans-4-Hydroxy-L-proline at Low Reaction Temperatures. *J. Am. Chem. Soc.* **2006**, *128*, 16050.
- Kündig, E. P.; Seidel, T. M.; Jia, Y.-x.; Bernardinelli, G. Bulky Chiral Carbene Ligands and Their Application in the Palladium-Catalyzed Asymmetric Intramolecular α -Arylation of Amides. *Angew. Chem., Int. Ed.* **2007**, *46*, 8484.
- García-Fortanet, J.; Buchwald, S. L. Asymmetric Palladium-Catalyzed Intramolecular α -Arylation of Aldehydes. *Angew. Chem., Int. Ed.* **2008**, *47*, 8108.
- Taylor, A. M.; Altman, R. A.; Buchwald, S. L. Palladium-Catalyzed Enantioselective α -Arylation and α -Vinylolation of Oxindoles Facilitated by an Axially Chiral P-Stereogenic Ligand. *J. Am. Chem. Soc.* **2009**, *131*, 9900.
- Würtz, S.; Lohre, C.; Fröhlich, R.; Bergander, K.; Glorius, F. IBiox[(-)-menthyl]: A Sterically Demanding Chiral NHC Ligand. *J. Am. Chem. Soc.* **2009**, *131*, 8344.
- Huang, Z.; Liu, Z.; Zhou, J. An Enantioselective, Intermolecular α -Arylation of Ester Enolates To Form Tertiary Stereocenters. *J. Am. Chem. Soc.* **2011**, *133*, 15882.
- Kobayashi, K.; Yamamoto, Y.; Miyaura, N. Pd/Josiphos-Catalyzed Enantioselective α -Arylation of Silyl Ketene Acetals and

Mechanistic Studies on Transmetalation and Enantioselection. *Organometallics* **2011**, *30*, 6323.

(30) Huang, Z.; Lim, L. H.; Chen, Z.; Li, Y.; Zhou, F.; Su, H.; Zhou, J. S. Arene CH-O Hydrogen Bonding: A Stereocontrolling Tool in Palladium-Catalyzed Arylation and Vinylation of Ketones. *Angew. Chem., Int. Ed.* **2013**, *52*, 4906.

(31) Huang, Z.; Chen, Z.; Lim, L. H.; Quang, G. C. P.; Hirao, H.; Zhou, J. S. Weak Arene C-H...O Hydrogen Bonding in Palladium-Catalyzed Arylation and Vinylation of Lactones. *Angew. Chem., Int. Ed.* **2013**, *52*, 5807.

(32) Cornella, J.; Jackson, E. P.; Martin, R. Nickel-Catalyzed Enantioselective C-C Bond Formation through C(sp²)-O Cleavage in Aryl Esters. *Angew. Chem., Int. Ed.* **2015**, *54*, 4075.

(33) Jiao, Z.; Beiger, J. J.; Jin, Y.; Ge, S.; Zhou, J. S.; Hartwig, J. F. Palladium-Catalyzed Enantioselective α -Arylation of α -Fluoroketones. *J. Am. Chem. Soc.* **2016**, *138*, 15980.

(34) Hao, Y.-J.; Hu, X.-S.; Zhou, Y.; Zhou, J.; Yu, J.-S. Catalytic Enantioselective α -Arylation of Carbonyl Enolates and Related Compounds. *ACS Catal.* **2019**, *10*, 955.

(35) Li, B.; Li, T.; Aliyu, M. A.; Li, Z. H.; Tang, W. Enantioselective Palladium-Catalyzed Cross-Coupling of α -Bromo Carboxamides and Aryl Boronic Acids. *Angew. Chem., Int. Ed.* **2019**, *58*, 11355.

(36) Jette, C. I.; Geibel, I.; Bachman, S.; Hayashi, M.; Sakurai, S.; Shimizu, H.; Morgan, J. B.; Stoltz, B. M. Palladium-Catalyzed Construction of Quaternary Stereocenters by Enantioselective Arylation of γ -Lactams with Aryl Chlorides and Bromides. *Angew. Chem., Int. Ed.* **2019**, *58*, 4297.

(37) He, Z.-T.; Hartwig, J. F. Palladium-Catalyzed α -Arylation of Carboxylic Acids and Secondary Amides via a Traceless Protecting Strategy. *J. Am. Chem. Soc.* **2019**, *141*, 11749.

(38) While writing this manuscript two articles were published that contained computational studies of racemic versions of α -arylations of carbonyl compounds: (a) Tcyrulnikov, S.; Kozlowski, M. C. Accounting for Strong Ligand Sensitivity in Pd-Catalyzed α -Arylation of Enolates from Ketones, Esters, and Nitroalkanes. *J. Org. Chem.* **2020**, *85*, 3465. (b) de Azambuja, F.; Yang, M.-H.; Feoktistova, T.; Selvaraju, M.; Brueckner, A. C.; Grove, M. A.; Koley, S.; Cheong, P. H.-Y.; Altman, R. A. Connecting remote C-H bond functionalization and decarboxylative coupling using simple amines. *Nat. Chem.* **2020**, *12*, 489.

(39) **8** is considered as the starting reactant rather than evaluating the thermodynamics of the transformation: $4a + tBuONa \rightarrow 8 + tBuOH$. We do so by virtue of the high experimental difference in pK_a^{DMSO} between **4a** (24–26, ref 39a) and $tBuONa$ (ca. 32, ref 39b) reported by Bordwell. Additionally, Na-enolates are known to produce higher order aggregates when generated quantitatively from a strong base. For simplicity, the monomeric Na-enolate **8** was used in this study. (a) Bordwell, F. G.; Cornforth, F. J. Application of the Hammett equation to equilibrium acidities of meta- and para-substituted acetophenones. *J. Org. Chem.* **1978**, *43*, 1763. (b) Olmstead, W. N.; Margolin, Z.; Bordwell, F. G. Acidities of water and simple alcohols in dimethyl sulfoxide solution. *J. Org. Chem.* **1980**, *45*, 3295.

(40) Orlandi, M.; Ceotto, M.; Benaglia, M. Kinetics versus thermodynamics in the proline catalyzed aldol reaction. *Chem. Sci.* **2016**, *7*, 5421.

(41) Seguin, T. J.; Lu, T.; Wheeler, S. E. Enantioselectivity in Catalytic Asymmetric Fischer Indolizations Hinges on the Competition of π -Stacking and CH/ π Interactions. *Org. Lett.* **2015**, *17*, 3066.

(42) Seguin, T. J.; Wheeler, S. E.; Wheeler, S. E. Competing Noncovalent Interactions Control the Stereoselectivity of Chiral Phosphoric Acid Catalyzed Ring Openings of 3-Substituted Oxetanes. *ACS Catal.* **2016**, *6*, 7222.

(43) Lu, G.; Liu, R. Y.; Yang, Y.; Fang, C.; Lambrecht, D. S.; Buchwald, S. L.; Liu, P. Ligand-Substrate Dispersion Facilitates the Copper-Catalyzed Hydroamination of Unactivated Olefins. *J. Am. Chem. Soc.* **2017**, *139*, 16548.

(44) Thomas, A. A.; Speck, K.; Kevlishvili, I.; Lu, Z.; Liu, P.; Buchwald, S. L. Mechanistically Guided Design of Ligands That

Significantly Improve the Efficiency of CuH-Catalyzed Hydroamination Reactions. *J. Am. Chem. Soc.* **2018**, *140*, 13976.

(45) Some of these contributions are intimately related and can be hardly separated. For instance, dissociation of the ligand from the metal center would allow for the evaluation of the ligand Pd bonds strength in principle. However, due to the significant distortion of the coordination sphere at the TS out of the square planar, this would result in a significant error. This error would originate from neglecting significant Pd orbitals rearrangement in the absence of the P atoms in the [Pd(Ph)(enolate)] fragment.

(46) Here we make an approximation by assuming that the (relative) interactions between the added H atoms and the reagents is negligible.

(47) Evaluation of $\Delta\Delta_{NCl}E^\ddagger$ between different TSs does not provide any insight about whether the energy difference is due to attractive or repulsive interactions. In order to prove that the NCIs in place are attractive, we performed the same energy decomposition analysis of Figure 4a between $TS_{RE}CR$ and (R)10 (ref 50). This allowed us to establish that NCIs contribute to the activation barrier by lowering its value with $\Delta_{NCl}E^\ddagger = -5.66$ kcal/mol.

(48) We chose to evaluate the distortion energy of the $PhPH_2$ group rather than PhH in order to include the C-P distortion energy into consideration. However, the results were shown to change only by hundredths of kcal/mol when compared to the use of the PhH truncation or even when neglecting the Ph portion distortion.

(49) Becke, A. D. Density-functional exchange-energy approximation with correct asymptotic behavior. *Phys. Rev. A: At., Mol., Opt. Phys.* **1988**, *38*, 3098.

(50) Perdew, J. P. Density-functional approximation for the correlation energy of the inhomogeneous electron gas. *Phys. Rev. B: Condens. Matter Mater. Phys.* **1986**, *33*, 8822.

(51) Perdew, J. P.; Burke, K.; Ernzerhof, M. Generalized gradient approximation made simple. *Phys. Rev. Lett.* **1996**, *77*, 3865.

(52) Cossi, M.; Rega, N.; Scalmani, G.; Barone, V. Energies, structures, and electronic properties of molecules in solution with the C-PCM solvation model. *J. Comput. Chem.* **2003**, *24*, 669.

(53) Knowles, R. R.; Jacobsen, E. N. Attractive noncovalent interactions in asymmetric catalysis: Links between enzymes and small molecule catalysts. *Proc. Natl. Acad. Sci. U.S.A.* **2010**, *107*, 20678.

(54) Grimme, S.; Antony, J.; Ehrlich, S.; Krieg, H. A consistent and accurate ab initio parameterization of density functional dispersion correction (DFT-D) for the 94 elements H-Pu. *J. Chem. Phys.* **2010**, *132*, 154104.